GSA Data Repository Item # 8524

Title of article Tectonic Relationships Between Forearc-Basin Strata and the Accretionary Complex at Bath, Barbados

Author(s) R. Torrini, Jr., Robert C. Speed, and G. S. Mattioli

see Bulletin v. 96, p. 861 - 874

Contents 20 pages

Appendix with figures

TECTONIC RELATIONSHIPS BETWEEN FOREARC BASIN STRATA AND THE ACCRETIONARY COMPLEX AT BATH, BARBADOS

Rudolph Torrini, Jr., Robert C. Speed, and Glen S. Mattioli

Department of Geological Sciences

Northwestern University

Evanston, Illinois 60201

APPENDIX

APPENDIX

This appendix contains the following structural, lithologic, and age data supplemental to Torrini and others (1985): (A) tabulated microfaunal dates of rocks in the Bath area (Fig. A1), (B) detailed fabric data and kinematic histories of radiolarite and hemipelagic rocks of the basal complex (Figs. A2 and A3), (C) fabric data and an outcrop sketch of melange body m_2 (Figs. A4 and A5), and (D) detailed outcrop sketches (Figs. A6-A10), tabulated microfaunal dates (Fig. A11), and lithologic characteristics (Fig. A12) of fault zone rocks in the sub-Oceanic fault zone (sofz) and hemipelagite/radiolarite fault zone (hrfz).

A) TABULATED MICROFAUNAL DATES

Figure A1 is a tabulation of radiolarian zonal assignments of pre-Pleistocene rocks of the Bath area. The numerical sequence beneath the zones (row marked by asterisk) is used as a code for dated sample sites shown in outcrop sketches (Figs. A6-A10). Columns contain the number of dated samples assigned to a given radiolarian zone; triangles indicate the number of dated samples that may possibly be assigned to the next youngest zone. The cross subscript (+; melange unit m_1) indicates uncertainty as to whether dated outcrop is a block in melange or adjacent wallrock. Dashed horizontal lines are ranges of ages obtained by foraminiferal dating. The cross-hatch symbol (#) indicates the presence of resedimented microfauna. Oceanic nappe o_7 contains resedimented foraminifera as old as middle Eocene; hemipelagic outcrop unit h_1 contains resedimented foraminifera and radiolaria of late Cretaceous age. Radiolarian zonal assignments were made by W. R. Riedel and A. B. Sanfilippo. Foraminiferal dates were assigned by J. B. Saunders. The correlation between microfaunal

zones and the time scale is from Berggren and others (1985).

B) RADIOLARITE AND HEMIPELAGIC ROCKS OF THE BASAL COMPLEX

Within the basal complex at Bath, radiolarite and hemipelagic rocks are structurally discrete from one another and were juxtaposed at a brittle fault zone (hrfz, Fig. A10) before emplacement of the Oceanic nappes. Structures within both suites indicate pre- and syn-SOFZ deformation. Both have early folds with subparallel west-plunging axes and axial planes that are girdled about the mean axis. Both underwent later low-angle fault imbrication related to emplacement of the Oceanic nappes and deformation by the syn-SOFZ major folds. The late major folds are approximately homoaxial to the early folds and caused partial girdling of the early axial planes.

Structure of Radiolarite: Four deformation phases are recognized in the radiolarite unit: 1) thrusting and probable isoclinal folding, 2) major and minor folding, 3) thrusting related to emplacement of the Oceanic nappes, and 4) folding of basal accretionary units and lower Oceanic nappes. All folds have axes that plunge shallowly west and shortening trends approximately north-south.

First phase thrusts are folded tabular zones of radiolarian mudstone breccia bounded by polished striated faults (Fig. A3). The zones, as thick as .3 m, contain spaced anastomosing cleavage that is increasingly penetrative close to faults. Like surrounding bedding, cleavage and faults are girdled about shallowly west-plunging axes (Fig. A2,a). Fault plane striae and slip directions calculated from local cleavage-fault pairs* are approximately colinear (Fig.

*Calculated slip directions assume that cleavage and fault displacement were contemporaneous plane strain features and that cleavage was normal to maximum shortening (Z). The slip lies in the projection of Z on the fault and is directed toward the Z-fault intersection.

A2,b), implying that cleavage, faults, and striae are kinematically related. they are first phase because cleavage is deformed by second phase folds. Southerly transport of hanging walls during early thrusting is indicated by all but one slip direction (Fig. A2,b) and presumably occurred either during initial accretion or intra-prism adjustments. Faunal ages within radiolarite packets indicate inversion of beds in locally homoclinal sections and thus, the existence of early isoclinal folds or bedding-parallel fault repetition. The absence of recognized fault-related structures makes the fold hypothesis more likely. The stratal inversions are considered first phase, but their timing relative to early thrusts is uncertain.

Second phase folds include a major fold couple that has a shallowly west-plunging axis and a sub-vertical ENE-striking axial plane (Fig. A2,c) (Fig. 4, Torrini and others, 1985). The fold couple has a wavelength of about 30 m, shape between chevron and sinusoidal, and near-parallel style. Axial plane cleavage is undetected. Radiolarite strata elsewhere in the packet assemblage are generally cylindrical with the fold couple (Fig. A2,d), suggesting homogeneous second phase deformation. Open minor chevron folds are common on the southern limb of the major synform. Bisecting planes of major and minor folds within the radiolarite unit, with one exception, are girdled about the cluster of fold axes (Fig. A2,e). The asymmetry of minor folds proximal to the major fold is consistent with a contemporaneous origin, but the large range of dips of the bisecting planes of the minor folds suggests somewhat earlier formation and rotation of the minor folds by the majors, or reorientation by late deformation.

Third phase thrusts juxtapose laminated and massive radiolarite and truncate the second phase major folds (D-D',Fig. 4, Torrini and others, 1985). An

age reversal exists across one of the thrusts. We relate such thrusts to the emplacement of one or more of the suprajacent Oceanic nappes because they have similar attitude ranges and slip directions (Fig. A2,f) to faults in the folded sub-Oceanic fault zone (Fig. 10a, Torrini and others, 1985).

The fourth phase of deformation generated the major SOFZ fold couple, following emplacement of the lower Oceanic nappes. Within the radiolarite packet assemblage, fourth phase structures include local minor folds of third phase thrusts (Fig. A2,g) (D-D', Fig. 4, Torrini and others, 1985), possible new thrusts (Fig. A2,g), and possible homoaxial refolding of second phase folds (Fig. A2,e). One chevron fold has a north-striking, subvertical axial plane and south-plunging axis (Fig. A2,h). Its proximity to the fault contact between the hemipelagite and radiolarite packet assemblages (hrfz, Fig. A10) suggests it was generated or reoriented by interpacket slip.

Structure of Hemipelagic Rocks: Hemipelagic strata crop out in five subaerial and subaquatic exposure areas (h_{1-5}, Fig. 4, Torrini and others, 1985) that include at least three fault-bounded packets. Outcrops h_1 and h_5 contain mappable folds that appear to record first deformation. Their axes plunge shallowly WNW (Figs. A2,i and j), but axial planes vary from subvertical to moderately southwest-dipping. Their shapes are between chevron and sinusoidal, styles parallel, and interlimb angles between 45° and 75°. Strata in outcrops h_{2-4} and away from folds in h_1 and h_5 (Figs. A2,k and l) are crudely girdled about mesoscopic fold axes. Outcrop h_2 contains upright beds that are older than but above beds of h_1, indicating fault juxtaposition. The timing between first folding and the inferred thrusting is uncertain.

Late deformation of the hemipelagite packet assemblage in the major fold couple that affects Oceanic nappes 1-4 is suggested by the outcrop distribution

of radiolarite and hemipelagic rocks (B-B', Fig. 4, Torrini and others, 1985). The different attitudes of axial planes of first folds in outcrops h_1 and h_5 may be related to this late, nearly homoaxial refolding. Late thrusting affected the hemipelagite packet assemblage at least at its southern reach, as indicated by imbricated hemipelagic rocks and Oceanic rocks as young as Miocene in the sub-Oceanic fault zone below Oceanic nappe 7 ($sofz_{6,7}$, Fig. A9).

C) MELANGE

Melange exists at Bath in two bodies ($m_{1,2}$, Fig. A4,a), both of which consist of cleaved, sandy, organic-rich mudstone that includes unsorted clasts up to 1 m long of tarry quartz sandstone, dolomitic mudstone, mudstone, micrite, and pebbly sandy micrite. Body m_2 is dike-like, southwest-dipping at 50°-60°, and 75-130 m thick. Its occurrence, indicated mainly by distinctive float and three excavated contacts (points a,b,c; Fig. A4,a) may be entirely with Oceanic nappe 6 or cut the 6-7 fault below thick cover. Thus, it is uncertain whether m_2 is allochthonous with nappe 6, or was emplaced in situ, before or after the arrival of nappe 7.

A diapiric origin of the melange bodies is probable because the melange cuts bedding and isochrons in nappe 6 and wallrock chalk is faulted and cleaved. A clast of micrite within m_2 contains middle Oligocene foraminifera that are older than Oceanic beds in the local walls (Fig. A5). Time lines and bedding in Oceanic nappe 6 (Fig. A4,b) suggest that m_2 was intruded without folding or faulting in the dike plane of the Oceanic host. Structures at the melange contacts, however, indicate local deformation during emplacement: faults, cleavage, and brecciation in chalk within 1 m of the contact, and cleavage, boudinage, and

alignment of faceted clasts in melange (Fig. A5). Faults and cleavage are parallel in chalk and melange (Figs. A4,c and A5), and boudin axes and maximum clast faces lie in the cleavage plane (Fig. A5). Cleavage deflects about clast tips. Although contacts are parallel, cleavage at points a and b (Fig. A4,c) differs in orientation. Calculated slip directions (Fig. A4,b) at both sites are scattered, implying either the existence of local rotations or that cleavage and faults are not kinematically related.

Body m_1 (Fig. A4,a), without exposed contacts, is of uncertain structural configuration with respect to its radiolarite host. Middle Eocene radiolarite in contacting outcrop (Fig. 4, Torrini and others, 1985) may be either an exceptionally large block or wall rock to the melange. By analogy with body m_2, we infer that m_1 is diapiric.

D) FAULT ZONE ROCKS

Figures A6-A10 are outcrop sketches of the sub-Oceanic fault zone (sofz) and hemipelagite/radiolarite fault zone (hrfz). The legend of symbols used in Figures A6-A9 is shown in Figure A6. Circled numbers in the sketches are coded radiolarian zonal assignments, keyed in Figure A11. The locations of the study sites ($sofz_{1-7}$; hrfz) in map and cross-section are in Figure 4 of Torrini and others (1985).

Figure A11 shows radiolarian zonal assignments of fault zone rocks. The numerical sequence (row marked by asterisk) is used as a code for dated sample sites in outcrop sketches (Figs. A6-A10). Letters in columns refer to the number of dates within a given subzone that are assigned to a given radiolarian zone. Dots are fault zones without subzone divisions. Plain letters or dots denote dated matrix; underlined letters or dots denote dated clasts. Triangle

superscripts indicate that samples may possibly be assigned to the next youngest zone. Dashed horizontal lines are foraminiferal dates by J. B. Saunders. Radiolarian zonal assignments were made by W. R. Riedel and A. B. Sanfilippo. The correlation between microfaunal zones and time scale is after Berggren and others (1985).

Figure A12 is a chart that tabulates lithologic data for the various subzones of the sofz study sites. X's refer to subzone matrix; solid triangles refer to subzone clasts. The relative abundance of organic carbon refers to the subzone as a whole.

REFERENCES CITED

Berggren, W. A., Kent, D. V., and Flynn, J. J., in press, Paleogene geochronology and chronostratigraphy, in Snelling, N.J., ed., Geochronology and the geological record: Geological Society of London Special Paper.

Torrini, R., Jr., Speed, R. C., and Mattioli, G., in press, Tectonic relationships between forearc basin strata and the accretionary complex at Bath, Barbados: Geological Society of America Bulletin.

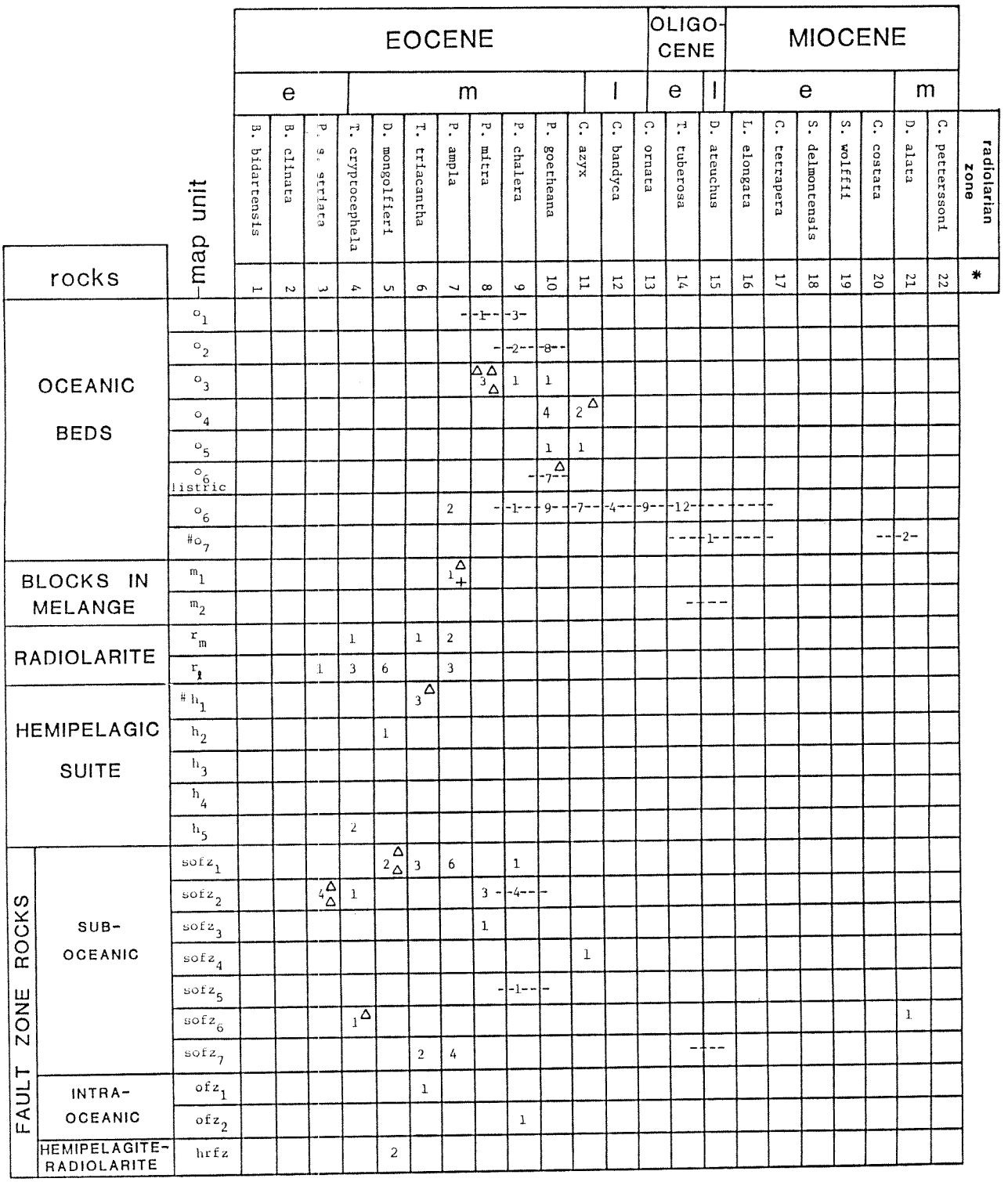
EOCENE
OLIGO-CENE
MIOCENE
e
m
l
e
l
e
m
B. bidartensis
B. clinata
P. g. striata
T. cryptocephela
D. mongolfieri
T. triacantha
P. ampla
P. mitra
P. chalera
P. goetheana
C. azyx
C. bandyca
C. ornata
T. tuberosa
D. ateuchus
L. elongata
C. tetrapera
S. delmontensis
S. wolffii
C. costata
D. alata
C. petterssoni
radiolarian zone
*
1
2
3
4
5
6
7
8
9
10
11
12
13
14
15
16
17
18
19
20
21
22
rocks
map unit
OCEANIC BEDS
BLOCKS IN MELANGE
RADIOLARITE
HEMIPELAGIC SUITE
FAULT ZONE ROCKS
SUB-OCEANIC
INTRA-OCEANIC
HEMIPELAGITE-RADIOLARITE

Figure A1

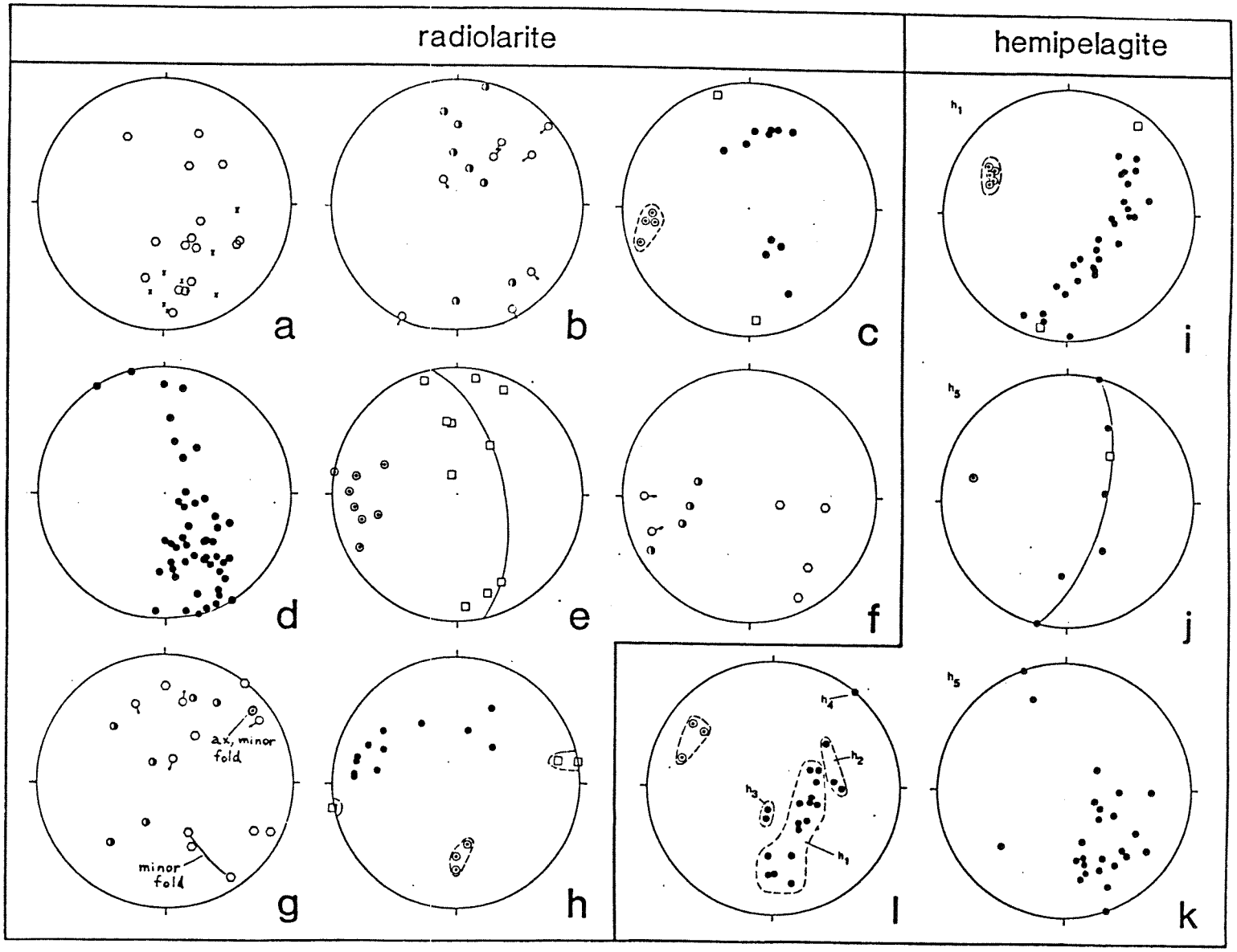
radiolarite
hemipelagite
a
b
c
d
e
f
g
h
i
j
k
l
ax, minor fold
minor fold
h1
h2
h3
h4
h5
pole to fault plane
pole to axial or bisecting plane
fault striation
pole to cleavage
pole to bedding: upright or attitude uncertain
calculated slipline
fold axis

Figure A2

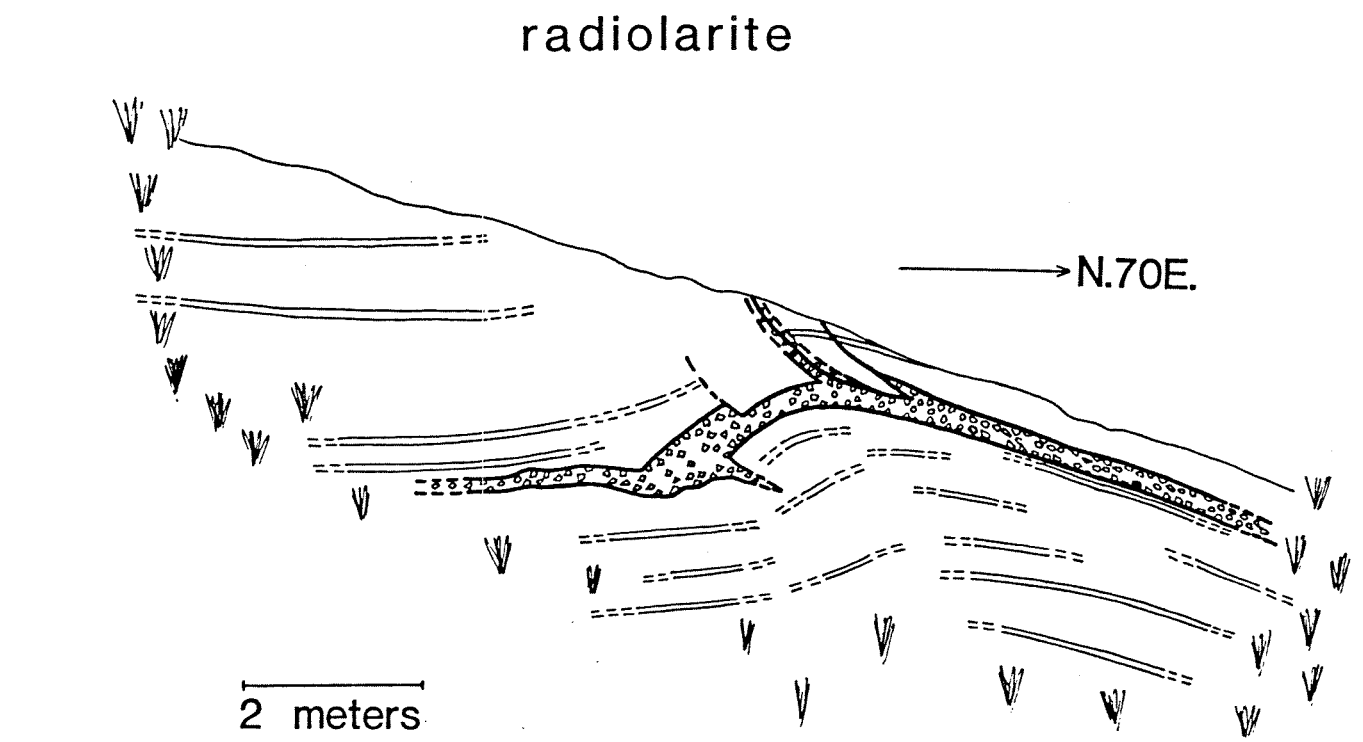

trace of bedding, laminated radiolarite

radiolarian mudstone breccia

Quaternary cover

Quaternary cover

fault, dashed where inferred

Figure A3

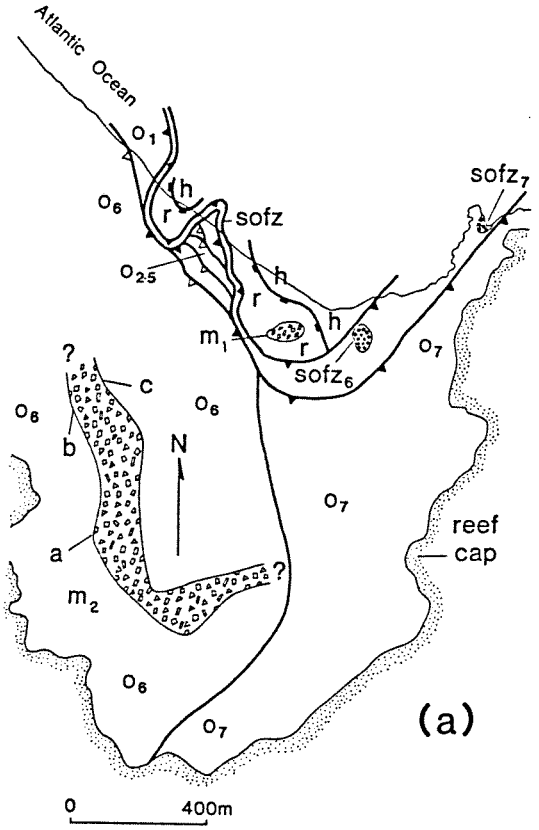

melange fabric data

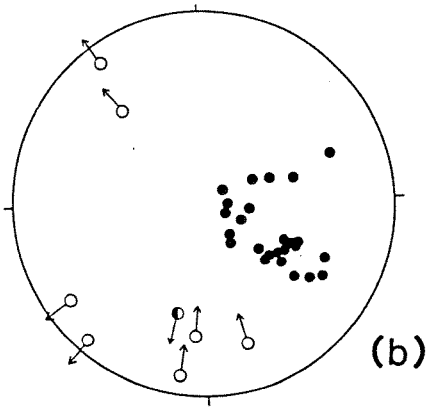

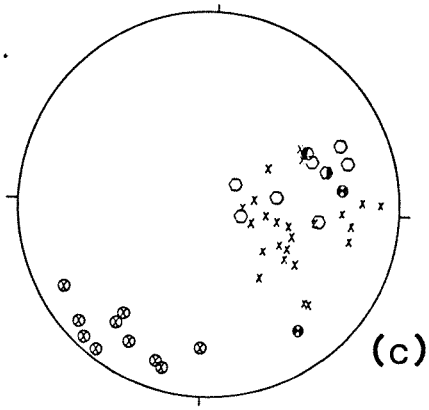

location (index map)	⊥ FAULTS	CALCULATED SLIPLINES	⊥ CLEAVAGE; MELANGE	⊥ CLEAVAGE; nappe o_6
point a	⬡	○→	X	⊖
point b	◐	◐→		⊗
point c	◑			

● ⊥ BEDDING; nappe o_6

Figure A4

melange/Oceanic contact (point a, Figure A4,a)

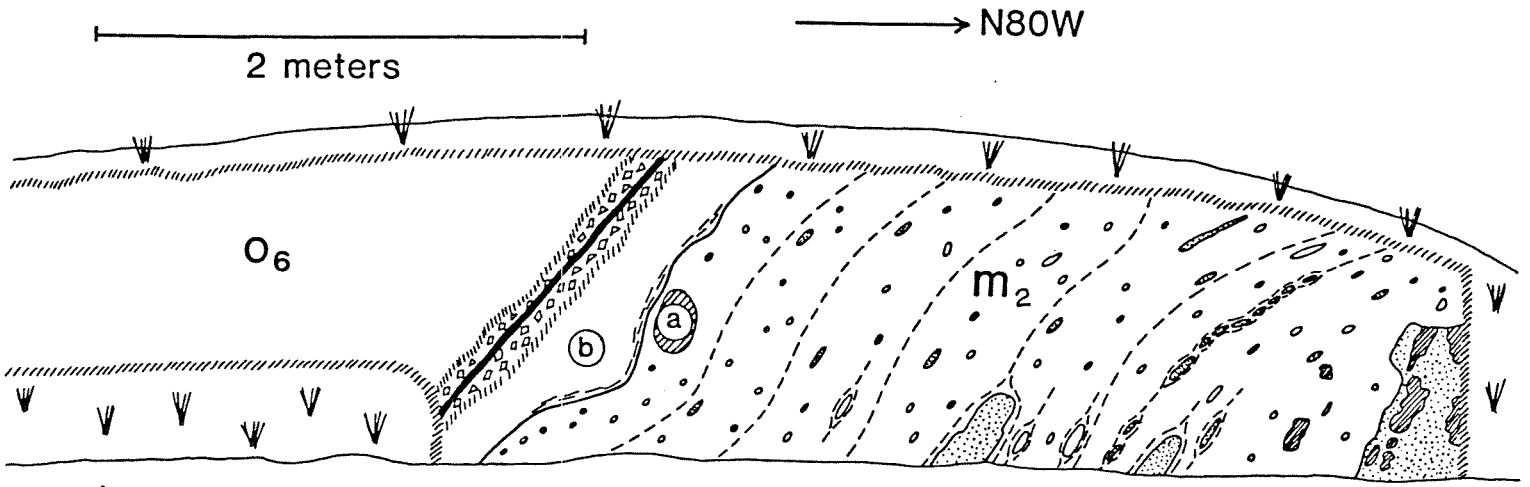

a) foram. date: early middle Oligocene

b) foram. date : late middle Oligocene

o_6 Oceanic nappe o_6

melange(diapir) m_2

chalk breccia

trace of cleavage

melange/o_6 contact

gradational contact

fault, dashed where inferred

Quaternary cover

Figure A5

$sofz_1$

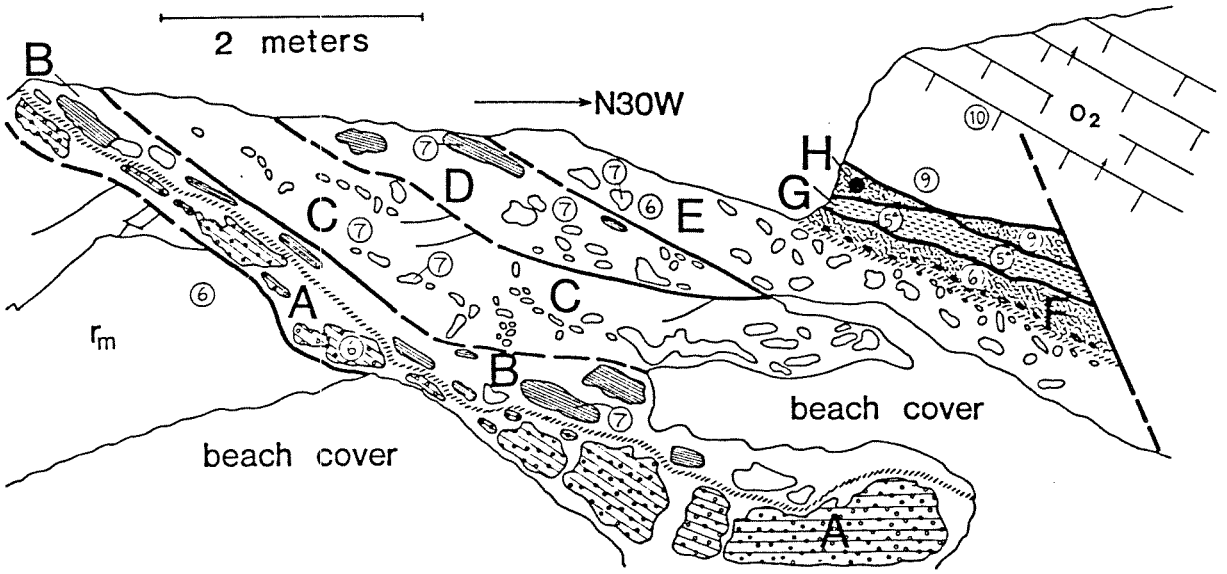

LEGEND: sub-Oceanic fault zone rocks

- radiolarian mudstone, massive or brecciated
- radiolarian mudstone, highly cleaved (brecciated in places)
- radiolarite, laminated
- rad-nanno marl breccia
- muddy radiolarite, massive or brecciated
- laminated radiolarian chert, hemipelagic
- hemipelagic radiolarian mudstone, massive
- foram-nanno chalk
- rad-nanno marl, arrows indicate facing evidence
- fault, dashed where inferred
- gradational contact
- Quaternary cover
- ② dated sample site with code number of radiolarian zone
- ● sample site, microfossils absent or poorly preserved
- lenticules of cleaved radiolarian mudstone with exotic clasts
- joints

nodule types

- limestone (ls)
- limestone, with relict sedimentary lamination
- laminated radiolarian chert

fault packet assemblages

- o_{1-6} Oceanic nappes
- $r_{m,l}$ radiolarite, m= massive, l= laminated

Figure A6

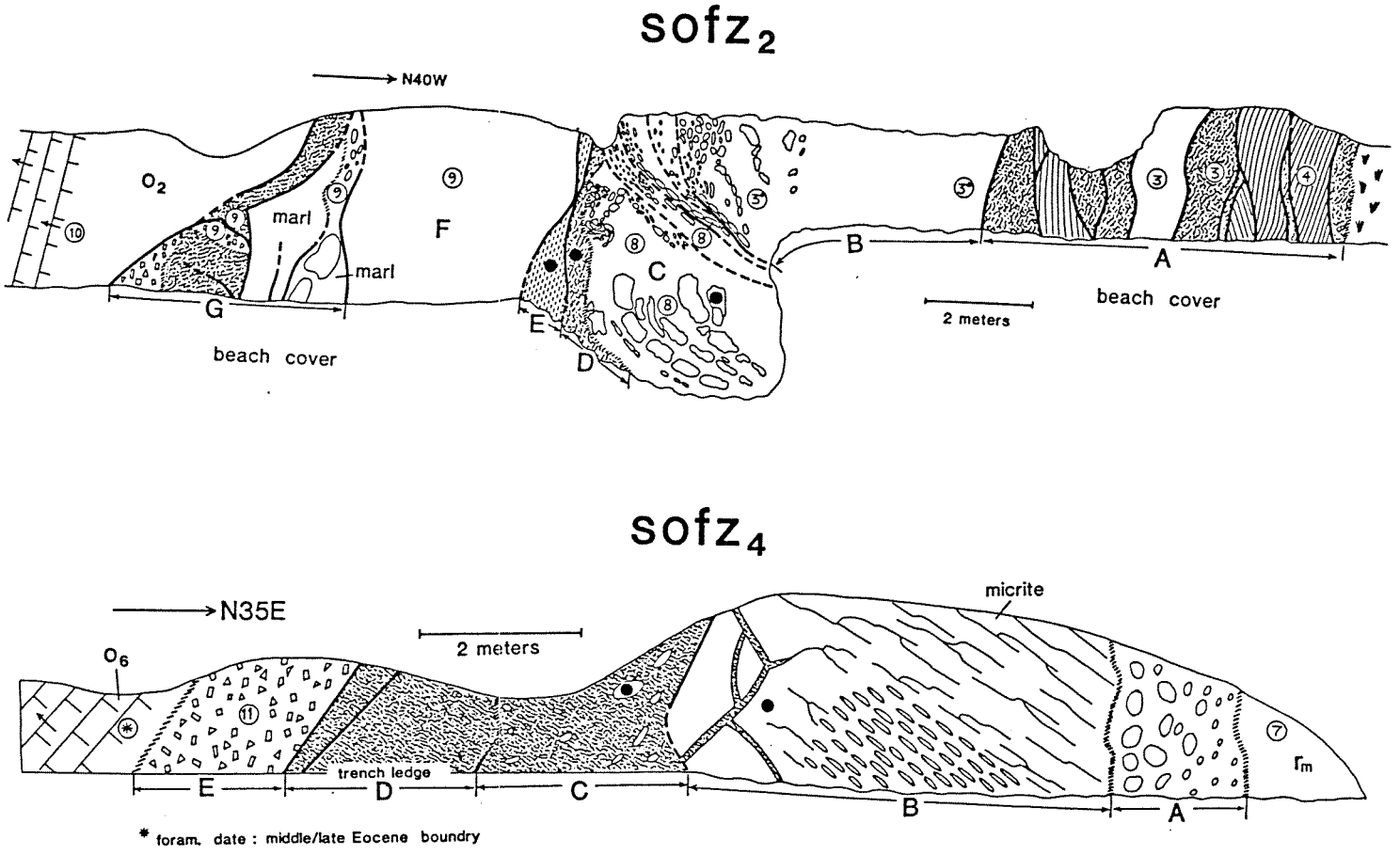
sofz2
N40W
O2
marl
marl
F
G
beach cover
E
D
C
B
A
2 meters
beach cover
sofz4
N35E
O6
2 meters
micrite
trench ledge
E
D
C
B
A
rm
* foram. date : middle/late Eocene boundry

Figure A7

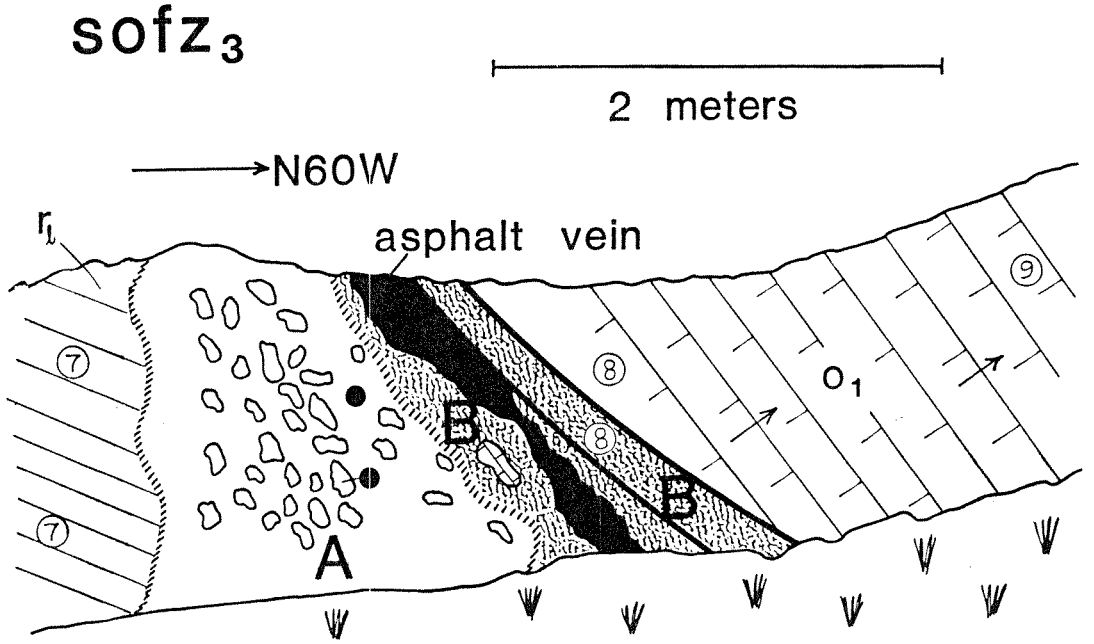
sofz3
2 meters
N60W
asphalt vein
r1
7
8
9
O1
A
B
B
B

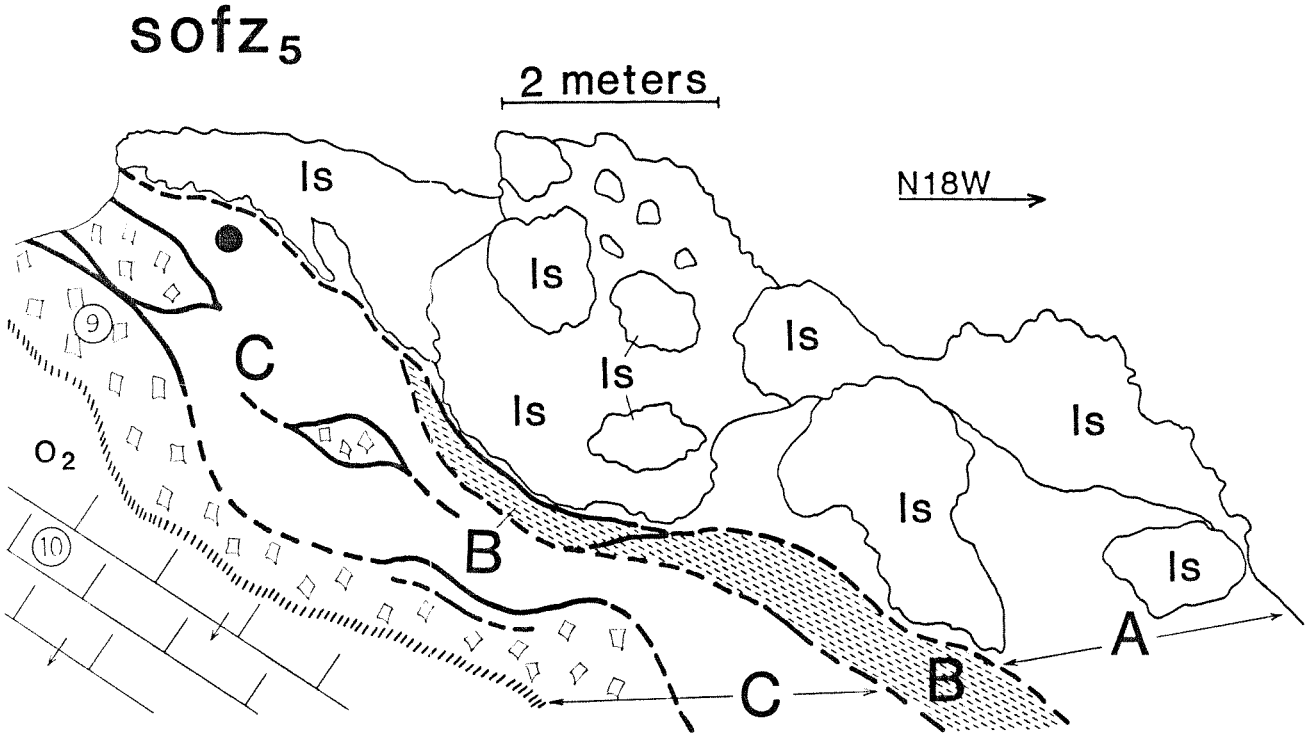
sofz5
2 meters
N18W
ls
ls
ls
ls
ls
ls
ls
ls
9
C
O2
10
B
C
B
A

Figure A8

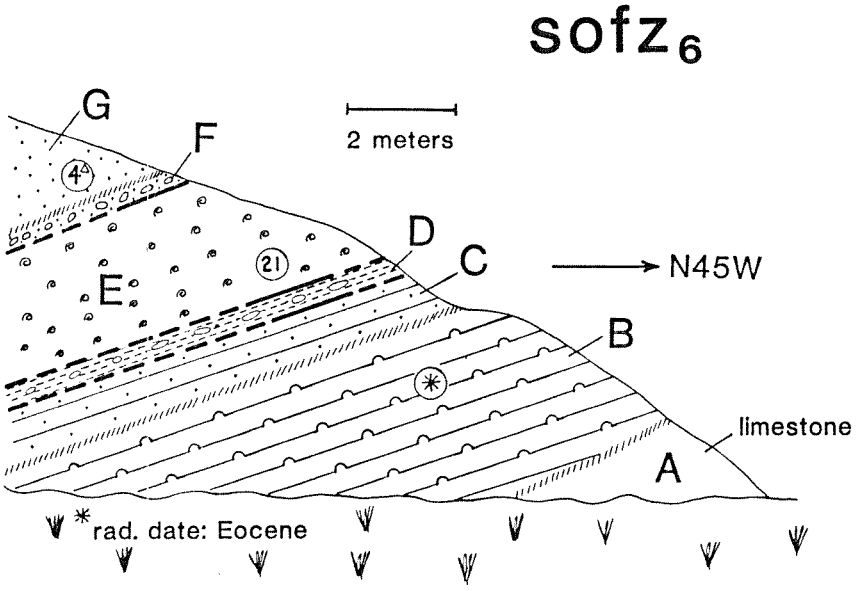
sofz6
G
F
2 meters
4a
D
C
21
E
N45W
B
limestone
A
* rad. date: Eocene

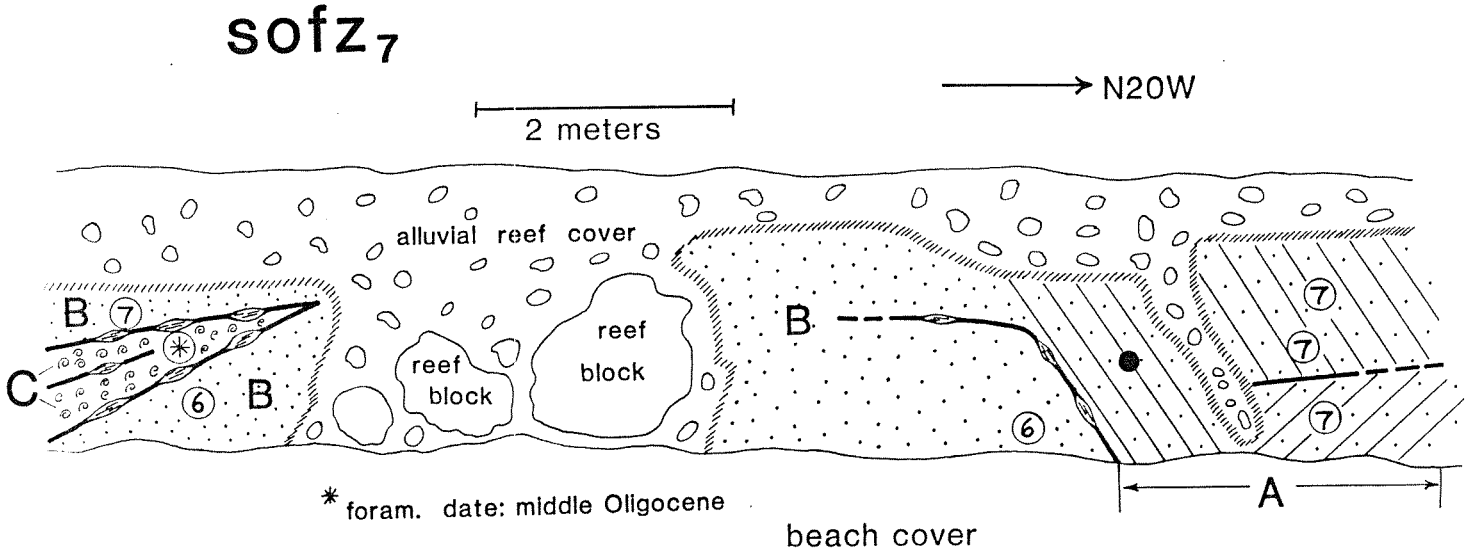
sofz7
N20W
2 meters
alluvial reef cover
B
7
C
6
B
reef block
reef block
B
7
7
7
6
A
* foram. date: middle Oligocene
beach cover

Figure A9

hemipelagite/radiolarite fault zone (hrfz)

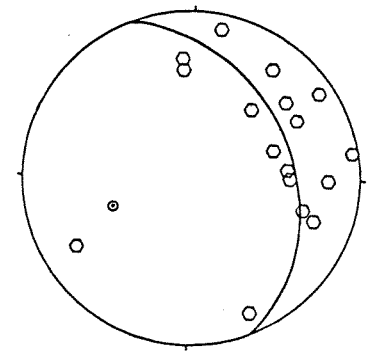

sedimentary lamination in blocks; subzone A

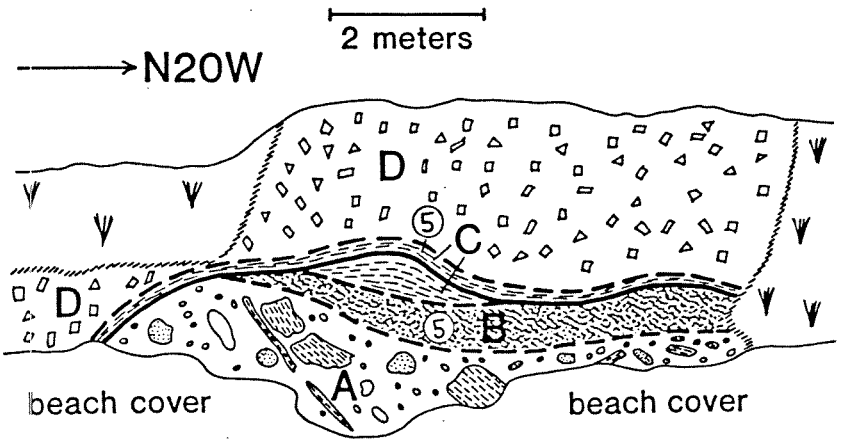

SUBZONE A — broken formation: mud pebbles, qtz. arenite clasts, and siltstone clasts in matrix of foliated clay

SUBZONE B — microbreccia: pebble-sized clasts of radiolarite, qtz. arenite, and green mudstone

SUBZONE C — cleaved microbreccia: dominantly pebble-sized mud clasts, along with minor radiolarite and qtz. arenite clasts

SUBZONE D — radiolarite breccia: framework of angular radiolarite clasts with matrix of radiolarian clay

fault, dashed where inferred

gradational contact

Quaternary cover

⑤ dated sample site

Figure A10

			EOCENE												OLIGO-CENE			MIOCENE						
			e			m							l		e	l		e					m	
			B. bidartensis	B. clinata	P. s. striata	T. cryptocephela	D. mongolfieri	T. triacantha	P. ampla	P. mitra	P. chalera	P. goetheana	C. azyx	C. bandyca	C. ornata	T. tuberosa	D. ateuchus	L. elongata	C. tetrapera	S. delmontensis	S. wolffii	C. costata	D. alata	C. pettersoni	radiolarian zone
			1	2	3	4	5	6	7	8	9	10	11	12	13	14	15	16	17	18	19	20	21	22	*
FAULT ZONE ROCKS	SUB-OCEANIC	$sofz_1$					G G	A E F	B C C D D E		H														
		$sofz_2$			A A B B	A				C C	C F G G														
		$sofz_3$								B															
		$sofz_4$											E												
		$sofz_5$									C														
		$sofz_6$				G																	E		
		$sofz_7$						B B	A A A B							C									
	INTRA-OCEANIC	ofz_1						●																	
		ofz_2									●														
	HEMIPELAGIC-RADIOLARITE	hrfz					BC																		

Figure A11

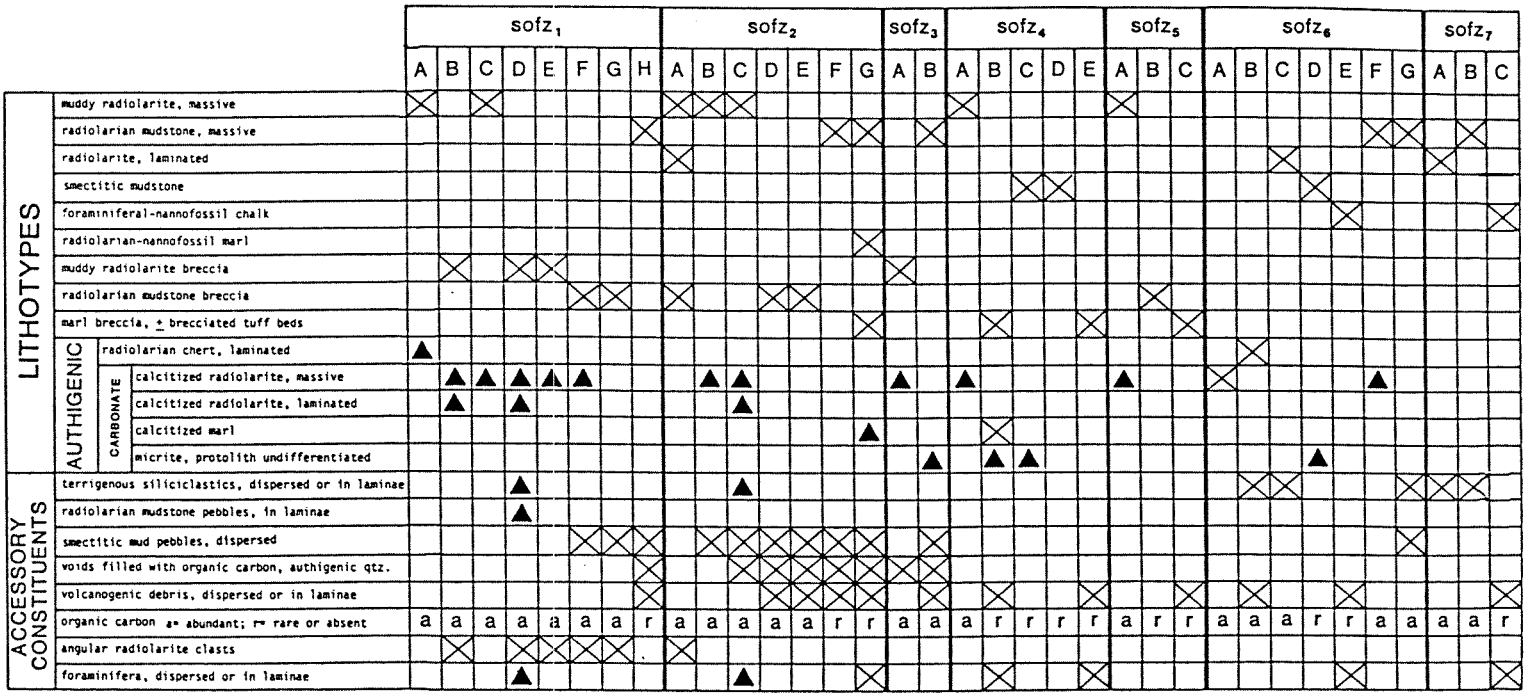
sofz1
sofz2
sofz3
sofz4
sofz5
sofz6
sofz7
A B C D E F G H
A B C D E F G
A B
A B C D E
A B C
A B C D E F G
A B C
LITHOTYPES
muddy radiolarite, massive
radiolarian mudstone, massive
radiolarite, laminated
smectitic mudstone
foraminiferal-nannofossil chalk
radiolarian-nannofossil marl
muddy radiolarite breccia
radiolarian mudstone breccia
marl breccia, ± brecciated tuff beds
AUTHIGENIC
radiolarian chert, laminated
CARBONATE
calcitized radiolarite, massive
calcitized radiolarite, laminated
calcitized marl
micrite, protolith undifferentiated
ACCESSORY CONSTITUENTS
terrigenous siliciclastics, dispersed or in laminae
radiolarian mudstone pebbles, in laminae
smectitic mud pebbles, dispersed
voids filled with organic carbon, authigenic qtz.
volcanogenic debris, dispersed or in laminae
organic carbon a= abundant; r= rare or absent
a a a a a a a r a a a a a r r a a a r r r r a r r a a a r r a a a r
angular radiolarite clasts
foraminifera, dispersed or in laminae

Figure A12